FG0287ER60512) for financial assistance. NMR spectra were obtained at the Washington University High-Resolution NMR Service Facility. This facility is funded in part by Biomedical Research Support Instrument Grant 1 S10 RR02004 and by a gift from the Monsanto Co. We thank Dr. Andrew Tyler of the Washington University Medical School for obtaining mass spectra of **1** and **2**. The Washington University Mass Spectrometry Resource is supported by a grant from the National Institutes of Health (RR00954). The MICROVAX Computer and Enraf-Nonius CAD4 diffractometer used in the structure determinations were purchased with National Science Foundation Grant CHE-8615556.

Supplementary Material Available: Listings of positional parameters, thermal parameters, crystallographic data, and bond distances and angles for **2** and **3** (18 pages); tables of F_o and F_c for **2** and **3** (27 pages). Ordering information is given on any current masthead page.

Contribution from the Department of Chemistry, Purdue University, West Lafayette, Indiana 47907

Reactions of the Polyhydride Complex $ReH_7(PPh_3)_2$ with Pyridinecarboxylic Acids, 2-Hydroxypyridine, 2-Hydroxy-6-methylpyridine, and Acetylacetone. Monohydrido Complexes of Rhenium(III) and Their Oxidation to the Corresponding Rhenium(IV) Derivatives

Phillip E. Fanwick, Malee Leeaphon, and Richard A. Walton*

Received June 19, 1989

The rhenium polyhydride complex $ReH_7(PPh_3)_2$ reacts with various organic acids to give neutral monohydrido rhenium(III) complexes of stoichiometry $ReH(L)_2(PPh_3)_2$, where L represents the monoanion of pyridine-2-carboxylic acid (pic), 1-isoquinolinecarboxylic acid (isoquin), pyridine-2,3-dicarboxylic acid (quin), 2-hydroxypyridine (hp), 2-hydroxy-6-methylpyridine (mhp), and acetylacetone (acac). These complexes display a reversible couple in their cyclic voltammograms (recorded in 0.1 M n-Bu_4NPF_6/CH_2Cl_2), which is associated with a one-electron oxidation to their 17-electron cations. The complexes where L = pic, isoquin, mhp, and acac have been oxidized to form their paramagnetic Re(IV) congeners $[ReH(L)_2(PPh_3)_2]PF_6$, using $[(\eta^5\text{-}C_5H_5)_2Fe]PF_6$ as the oxidant. These are rare examples of mononuclear Re(IV) hydride complexes; their reduction back to the neutral Re(III) precursors has been accomplished with the use of $(\eta^5\text{-}C_5H_5)_2Co$. The complexes $[ReH(pic)_2(PPh_3)_2]PF_6$ (**1**), $ReH(acac)_2(PPh_3)_2$ (**2**), and $[ReH(acac)_2(PPh_3)_2]PF_6$ (**3**) have been structurally characterized by X-ray crystallography. Crystal data for **1** at 20 °C: space group $C2/c$, a = 18.730 (5) Å, b = 19.877 (2) Å, c = 24.355 (4) Å, β = 90.46 (2)°, V = 9066 (5) Å^3, and Z = 8. The structure was refined to R = 0.036 and R_w = 0.041 for 3814 data with $I > 3.0\sigma(I)$. Crystal data for **2** at 20 °C: space group $P\bar{1}$, a = 11.892 (3) Å, b = 12.436 (2) Å, c = 15.713 (4) Å, α = 90.45 (2)°, β = 98.21 (2)°, γ = 115.53 (2)°, V = 2069 (2) Å^3, and Z = 2. The structure was refined to R = 0.032 and R_w = 0.042 for 4920 data with $I > 3\sigma(I)$. Crystal data for **3** at 21 °C: space group $P2_1/c$, a = 10.644 (3) Å, b = 19.803 (4) Å, c = 21.298 (6) Å, β = 92.48 (2)°, V = 4485 (4) Å^3, and Z = 4. The structure was refined to R = 0.051 and R_w = 0.060 for 4088 data with $I > 3.0\sigma(I)$. All three complexes have closely similar structures, which can be described in terms of distorted-pentagonal-bipyramidal or capped-octahedral geometries. Only in the case of **2** was the hydride ligand located in the structure analysis. The Re-H distance in **2** is 1.54 (5) Å.

Introduction

The treatment of the mononuclear polyhydride complexes $ReH_7(PPh_3)_2$ and $ReH_5(PPh_3)_2L$ (L = py, $C_6H_{11}NH_2$, t-$BuNH_2$) with $HBF_4\cdot Et_2O$ in acetonitrile or propionitrile results in the loss of H_2 and the formation of the seven-coordinate monohydridorhenium(III) complexes $[ReH(NCR)_3L(PPh_3)_2](BF_4)_2$ (R = CH_3, C_2H_5; L = CH_3CN, C_2H_5CN, py, $C_6H_{11}NH_2$, t-$BuNH_2$).[1] While electrochemical measurements (cyclic voltammetry) on solutions of these complexes in 0.1 M n-Bu_4NPF_6/CH_2Cl_2 showed that they possess a reversible one-electron oxidation in the potential range +1.0 to +1.6 V (vs Ag/AgCl), we were not successful in isolating samples of the paramagnetic rhenium(IV) species $[ReH(NCR)_3L(PPh_3)_2]^{3+}$. By reverting to organic ligands that both serve as monoprotic acids toward $ReH_7(PPh_3)_2$, with the release of H_2, and give rise to bidentate monoanionic ligands that help stabilize the resulting lower valent rhenium hydride species, we have succeeded in isolating neutral seven-coordinate monohydrido rhenium(III) complexes of the type $ReH(L)_2(PPh_3)_2$, where L is the monoanion of pyridine-2-carboxylic acid (pic), 1-isoquinolinecarboxylic acid (isoquin), pyridine-2,3-dicarboxylic acid (quin), 2-hydroxypyridine (hp), 2-hydroxy-6-methylpyridine (mhp), or acetylacetone (acac). In several instances, these complexes have been oxidized to their rhenium(IV) congeners; these constitute rare examples of *mononuclear* rhenium(IV) hydride complexes.[2,3] The synthesis and characterization of these complexes is described in this report, including details of the X-ray crystal structures of $[ReH(pic)(PPh_3)_2]PF_6$, and the redox pair $ReH(acac)_2(PPh_3)_2$ and $[ReH(acac)_2(PPh_3)_2]PF_6$.

Experimental Section

Starting Materials. The polyhydride complexes $ReH_7(PPh_3)_2$, $ReH_5(PPh_3)_3$, and $ReH_5(PPh_3)_2(py)$ were prepared by standard literature methods.[4] Cobaltocene was obtained from Strem Chemicals while $[(\eta^5\text{-}C_5H_5)_2Fe]PF_6$ was prepared as described in the literature.[5] Other reagents and solvents were obtained from commercial sources. Solvents were thoroughly deoxygenated prior to use.

Reaction Procedures. All reactions were performed under an atmosphere of dry nitrogen.

A. Reactions of $ReH_7(PPh_3)_2$ with Pyridinecarboxylic Acids. (i) $ReH(pic)_2(PPh_3)_2\cdot H_2O$. A slurry of $ReH_7(PPh_3)_2$ (0.100 g, 0.14 mmol) and pyridine-2-carboxylic acid (0.034 g, 0.28 mmol) in 5 mL of ethanol was refluxed for 20 min. Diethyl ether (100 mL) was added to the cooled reaction mixture, and the dark red solution was stirred for 5 min. A red

(1) Allison, J. D.; Moehring, G. A.; Walton, R. A. *J. Chem. Soc., Dalton Trans.* **1986**, 67.

(2) Conner, K. A.; Walton, R. A. In *Comprehensive Coordination Chemistry*; Wilkinson, G., Ed.; Pergamon: Oxford, England, 1987; Chapter 43, p 174.

(3) There are of course several examples of dinuclear rhenium(IV) hydrides of the type $Re_2H_8(PR_3)_4$; see: ref 2, pp 174-175.

(4) Chatt, J.; Coffey, R. S. *J. Chem. Soc. A* **1969**, 1963.

(5) Fanwick, P. E.; Harwood, W. S.; Walton, R. A. *Inorg. Chim. Acta* **1986**, *122*, 7.

0020-1669/90/1329-0676$02.50/0

precipitate was filtered off, washed with diethyl ether, and dried under vacuum; yield 0.095 g (71%). Anal. Calcd for $C_{48}H_{41}N_2O_5P_2Re$: C, 59.18, H, 4.25. Found: C, 58.70; H, 4.14.

(ii) $ReH(isoquin)_2(PPh_3)_2 \cdot H_2O$. A slurry of $ReH_7(PPh_3)_2$ (0.10 g, 0.14 mmol) and 1-isoquinolinecarboxylic acid (0.09 g, 0.28 mmol) in 5 mL of ethanol was refluxed for 20 min. The dark purple insoluble product was filtered off and dried under vacuum; yield 75%. Anal. Calcd for $C_{56}H_{49}N_2O_5P_2Re$: C, 62.61; H, 4.61. Found: C, 62.68; H, 4.89.

(iii) $ReH(quin)_2(PPh_3)_2 \cdot H_2O$. A procedure similar to that described in section A(ii) was used. The dark purple product was dried under vacuum; yield 70%. Anal. Calcd for $C_{50}H_{49}N_2O_5P_2Re$: C, 56.59; H, 3.81. Found: C, 56.28; H, 3.62.

B. Reactions of $ReH_7(PPh_3)_2$ with 2-Hydroxypyridines. (i) $ReH(hp)_2(PPh_3)_2 \cdot 2H_2O$. A mixture of $ReH_7(PPh_3)_2$ (0.200 g, 0.279 mmol) and 2-hydroxypyridine (0.106 g, 1.11 mmol) in 5 mL of acetone was refluxed for 30 min. A large excess of methanol (100 mL) was added to the cooled reaction mixture, and the orange solution was stirred for 5 min. The orange precipitate was filtered off, washed with methanol, and dried under vacuum; yield 0.220 g (88%). Anal. Calcd for $C_{46}H_{43}N_2O_4P_2Re$: C, 59.01; H, 4.64. Found: C, 59.11; H, 4.72.

(ii) $ReH(mhp)_2(PPh_3)_2 \cdot H_2O$. A mixture of $ReH_7(PPh_3)_2$ (0.300 g, 0.418 mmol) and 2-hydroxy-6-methylpyridine (0.140 g, 1.255 mmol) in 5 mL of acetone was refluxed for 30 min. Workup as in section B(i) gave an orange precipitate that was filtered from the cooled reaction mixture and dried under vacuum; yield 0.350 g (90%). Anal. Calcd for $C_{48}H_{45}N_2O_3P_2Re$: C, 60.93; H, 4.80. Found: C, 60.35; H, 4.73.

C. Reaction of $ReH_7(PPh_3)_2$ with Acetylacetone. $ReH(acac)_2(PPh_3)_2 \cdot H_2O$. Acetylacetone (0.40 mL, 3.9 mmol) was added to a slurry of $ReH_7(PPh_3)_2$ (0.200 g, 0.278 mmol) in 5 mL of ethanol. The mixture was refluxed for 12 min. The resulting dark red solution was cooled to room temperature to allow the precipitation of the red-brown product. The solid was filtered off and dried under vacuum; yield 0.180 g (83%). Anal. Calcd for $C_{46}H_{47}O_5P_2Re$: C, 59.53; H, 5.12. Found: C, 59.84; H, 5.27.

D. Oxidation of $ReH(L)_2(PPh_3)_2$ (L = pic, isoquin, hp, mhp, acac) with $[(\eta^5\text{-}C_5H_5)_2Fe]PF_6$. (i) $[ReH(pic)_2(PPh_3)_2]PF_6$. A solution of $ReH(pic)_2(PPh_3)_2$ (0.060 g, 0.063 mmol) and $[(\eta^5\text{-}C_5H_5)_2Fe]PF_6$ (0.021 g, 0.063 mmol) in 5 mL of acetone was stirred for 30 min. Diethyl ether (50 mL) was added to the solution to precipitate the orange product; yield 0.060 g (87%).

A similar procedure to this was used to prepare other oxidized Re(IV) species, the only exceptions being $[ReH(quin)_2(PPh_3)_2]PF_6$ and $[ReH(hp)_2(PPh_3)_2]PF_6$, neither of which were isolated in a pure state by this means (see Results and Discussion).

(ii) $[ReH(isoquin)_2(PPh_3)_2]PF_6 \cdot 2H_2O$: dark blue solid; yield 63%. *Anal.* Calcd for $C_{56}H_{47}N_2F_6O_4P_3Re$: C, 53.58; H, 3.94. Found: C, 53.69; H, 3.81.

(iii) $[ReH(mhp)_2(PPh_3)_2]PF_6$: dark blue solid; yield 95%.

(iv) $[ReH(acac)_2(PPh_3)]PF_6$: dark red solid; yield 81%.

This complex is also formed by air oxidation of the neutral precursor. A solution containing $ReH(acac)_2(PPh_3)_2$ (0.050 g, 0.055 mmol) and 1 equiv of KPF_6(0.01 g, 0.055 mmol) in ethanol (5 mL), was stirred in air for 10 min. Diethyl ether (50 mL) was added to the mixture to precipitate this product, yield 0.030 g (52%).

The identity of the products in sections D(i)–D(iv) was based upon their spectroscopic and electrochemical data and elemental microanalyses and, in the case of $[ReH(pic)_2(PPh_3)_2]PF_6$ and $[ReH(acac)_2(PPh_3)_2]PF_6$, upon single-crystal X-ray structure analyses.

E. Reduction of $[ReH(L)_2(PPh_3)_2]PF_6$ (L = pic, isoquin, mhp, acac) with $(\eta^5\text{-}C_5H_5)_2Co$. (i) $ReH(pic)_2(PPh_3)_2$. A solution of $[ReH(pic)_2(PPh_3)_2]PF_6$ (0.060 g, 0.054 mmol) and $(\eta^5\text{-}C_5H_5)_2Co$ (0.010 g, 0.054 mmol) in 5 mL of acetone was stirred for 20 min. Diethyl ether (50 mL) was added to the solution to precipitate the product; yield 0.040 g (77%).

Similar procedures were used to reduce the other complexes listed in section D.

(ii) $ReH(isoquin)_2(PPh_3)_2$: yield 70%.

(iii) $ReH(mhp)_2(PPh_3)_2$: yield 67%.

(iv) $ReH(acac)_2(PPh_3)_2$: yield 75%.

In all instances, these products were identified on the basis of their spectroscopic and electrochemical properties.

Preparation of Single Crystals for Structure Determinations. Crystals of $[ReH(pic)_2(PPh_3)_2]PF_6$ were grown through the use of a slow diffusion technique whereby deoxygenated heptane was layered onto a dilute solution of this complex in 1,2-dichloroethane. In a similar manner, crystals of $ReH(acac)_2(PPh_3)_2$ were grown by the slow diffusion of deoxygenated ethanol into a dilute solution in THF, while crystals of $[ReH(acac)_2(PPh_3)_2]PF_6$ were grown from deoxygenated heptane/THF.

X-ray Crystallography. The structures of $[ReH(pic)_2(PPh_3)_2]PF_6$ (**1**), $ReH(acac)_2(PPh_3)_2$ (**2**), and $[ReH(acac)_2(PPh_3)_2]PF_6$ (**3**) were determined by application of the general procedures that are described more fully elsewhere.[5] For convenience, these complexes will be denoted as **1–3**, respectively, in all further discussions of their crystallographic properties. The basic crystallographic parameters for these three complexes are listed in Table I. The cell constants are based on 25 reflections with $16.2 < \theta < 18.6°$ for **1**, $21.0 < \theta < 23.0°$ for **2**, and $15.6 < \theta < 18.2°$ for **3**. Three standard reflections were measured after 5000-s of beam time during data collection.

Table I. Crystallographic Data for $[ReH(pic)_2(PPh_3)_2]PF_6$ (**1**), $ReH(acac)_2(PPh_3)_2$ (**2**), and $[ReH(acac)_2(PPh_3)_2]PF_6$ (**3**)

	1	**2**	**3**
chemical formula	$ReP_3F_6O_4N_2C_{48}H_{39}$	$ReP_2O_4C_{46}H_{45}$	$ReP_3F_6O_4C_{46}H_{45}$
a, Å	18.730 (5)	11.892 (3)	10.644 (3)
b, Å	19.877 (2)	12.436 (2)	19.803 (4)
c, Å	24.355 (4)	15.713 (4)	21.298 (6)
α, deg	90	90.45 (2)	
β, deg	90.46 (2)	98.21 (2)	92.48 (2)
γ, deg	90	115.53 (2)	
V, Å^3	9066 (5)	2069 (2)	4485 (4)
Z	8	2	4
fw	1100.97	910.02	1054.98
space group	$C2/c$ (No. 15)	$P\bar{1}$ (No. 2)	$P2_1/c$ (No. 14)
T, °C	20	20	21
radiation (λ, Å)	Mo Kα (0.71073)	Mo Kα (0.71073)	Mo Kα (0.71073)
ρ_{calcd}, g cm^{-3}	1.613	1.461	1.555
μ(Mo Kα), cm^{-1}	28.89	30.91	29.05
transm coeff	1.000–0.529	1.000–0.807	1.000–0.549
R^a	0.036	0.032	0.051
$R_w{}^b$	0.041	0.042	0.060

$^a R = \sum||F_o| - |F_c||/\sum|F_o|$. $^b R_w = \{\sum w(|F_o| - |F_c|)^2/\sum w|F_o|^2\}^{1/2}$; $w = 1/\sigma^2(|F_o|)$.

Calculations were performed on a MicroVAX II computer using the Enraf-Nonius structure determination package. The structures were solved by the use of the Patterson heavy-atom method, which revealed the positions of the Re atoms. The remaining atoms were located in succeeding difference Fourier syntheses. Lorentz and polarization corrections were applied to the data. In all instances, an empirical absorption correction was applied,[6] the linear absorption coefficients being 28.89 cm^{-1} (for **1**), 30.91 cm^{-1} (for **2**), and 29.05 cm^{-1} (for **3**). No corrections for extinction were applied. The structures were refined by full-matrix least-squares methods where the function minimized was $\sum w(|F_o| - |F_c|)^2$ where w is the weighting factor defined as $w = 1/\sigma^2(F_o)$.

For structures of the hexafluorophosphate salts **1** and **3**, the positions for the hydrogen atoms of the pic, acac, and PPh_3 ligands were calculated by assuming idealized geometry and a C–H bond distance of 0.95 Å. For the methyl groups of the acac ligands, one hydrogen was located in a difference Fourier map, its position was idealized, and the remaining positions were calculated. We assumed that the value of B(H), i.e. the isotopic equivalent thermal parameter for the hydrogen atoms, was equal to $1.3[B_{eqv}(C)]$ at the time of the inclusion of this parameter in the refinement procedure. While these hydrogen atoms were used in the calculation of F_o, they were not included in the least-squares refinement. All non-hydrogen atoms of **1** and **3** were refined anisotropically; corrections for anomalous scattering were applied to these atoms.[7] The largest peak in the final difference Fourier map for **1** was 0.79 e Å^{-3} while for **3** it was 2.20 e Å^{-3}; the latter was located at non-bonding distances to the cation and anion and may be associated with lattice solvent although no attempt was made to model it in this fashion. It did not appear to be of any special chemical significance.

In the case of **2**, the crystal selected proved to be of very good quality and afforded an excellent data set with 4920 of the 5391 data collected being used in the refinement. The likely position of the hydride ligand was revealed in a difference Fourier map. It was refined on this assumption to give a very acceptable Re–H distance (1.54 (5) Å). With only isotropic refinement of the non-hydrogen atoms the residue was already 0.032 (R_w = 0.042). At this stage, the largest peak in the difference Fourier map was 0.71 e Å^{-3} and no spurious peaks were found about the Re atom. Since the refinement had already proceeded to a perfectly acceptable stage, we chose not to refine these atoms anisotropically. As in the case of **3**, the positions for the hydrogen atoms of

(6) Walker, N.; Stuart, D. *Acta Crystallogr., Sect. A: Found. Crystallogr.* **1983**, *A39*, 158.

(7) (a) Cromer, D. T. *International Tables for X-ray Crystallography*; Kynoch: Birmingham, England, 1974; Vol. IV, Table 2.3.1. (b) For the scattering factors used in the structure solution see Cromer, D. T.; Waber, J. T. *Ibid.*; Table 2.2B.

Table II. Positional Parameters and Equivalent Isotropic Displacement Parameters for Non-Phenyl Atoms of **1** and Their Estimated Standard Deviations

atom	*x*	*y*	*z*	*B*,[a] Å^2
Re	0.23594 (2)	0.05667 (2)	0.09698 (1)	2.741 (6)
P(1)	0.1343 (1)	0.0463 (1)	0.15918 (9)	3.03 (5)
P(2)	0.3561 (1)	0.0349 (1)	0.13393 (9)	2.90 (5)
O(171)	0.1547 (3)	0.0892 (3)	0.0450 (2)	3.5 (1)
O(172)	0.1127 (4)	0.1792 (4)	0.0009 (3)	7.2 (2)
O(271)	0.2942 (3)	0.0777 (3)	0.0274 (2)	3.8 (1)
O(272)	0.3144 (4)	0.0463 (4)	−0.0589 (2)	5.7 (2)
N(11)	0.2382 (4)	0.1621 (3)	0.1083 (2)	2.9 (2)
N(21)	0.2261 (4)	−0.0341 (3)	0.0510 (3)	3.3 (2)
C(12)	0.1966 (5)	0.1963 (5)	0.0712 (4)	3.7 (2)
C(13)	0.1960 (6)	0.2664 (5)	0.0686 (4)	5.1 (3)
C(14)	0.2378 (6)	0.3026 (5)	0.1046 (5)	5.7 (3)
C(15)	0.2781 (6)	0.2680 (5)	0.1429 (4)	4.9 (3)
C(16)	0.2775 (5)	0.1991 (5)	0.1444 (4)	4.0 (2)
C(17)	0.1516 (5)	0.1532 (5)	0.0352 (4)	4.5 (2)
C(22)	0.2541 (6)	−0.0298 (5)	0.0004 (4)	4.2 (2)
C(23)	0.2488 (7)	−0.0822 (5)	−0.0373 (4)	5.4 (3)
C(24)	0.2163 (8)	−0.1413 (6)	−0.0223 (5)	6.8 (3)
C(25)	0.1900 (7)	−0.1466 (5)	0.0301 (5)	5.9 (3)
C(26)	0.1953 (5)	−0.0931 (5)	0.0661 (4)	4.4 (2)
C(27)	0.2900 (5)	0.0354 (5)	−0.0130 (4)	4.1 (2)
P(100)	0.2633 (2)	0.2478 (2)	0.3211 (1)	5.12 (7)
F(101)	0.2212 (5)	0.2934 (5)	0.2808 (4)	14.5 (3)
F(102)	0.3082 (4)	0.2027 (5)	0.3606 (3)	10.0 (2)
F(103)	0.2171 (5)	0.2668 (6)	0.3704 (4)	15.0 (3)
F(104)	0.3119 (7)	0.2277 (6)	0.2744 (3)	16.8 (4)
F(105)	0.2158 (6)	0.1894 (5)	0.3095 (5)	18.4 (4)
F(106)	0.3119 (6)	0.3065 (5)	0.3339 (4)	15.5 (4)

[a] Values for anisotropically refined atoms are given in the form of the isotropic equivalent thermal parameter defined as $(4/3)[a^2B(1,1) + b^2B(2,2) + c^2B(3,3) + ab(\cos\gamma)B(1,2) + ac(\cos\beta)B(1,3) + bc(\cos\alpha)B(2,3)]$. Data for the phenyl atoms are available as supplementary material.

Table III. Positional Parameters and Equivalent Isotropic Displacement Parameters for Non-Phenyl Atoms of **2** and Their Estimated Standard Deviations

atom	*x*	*y*	*z*	*B*,[a] Å^2
Re	0.22093 (2)	0.20664 (2)	0.27043 (1)	2.428 (4)
P(1)	0.3335 (1)	0.1290 (1)	0.36361 (9)	2.64 (2)
P(2)	0.3473 (1)	0.3251 (1)	0.17433 (9)	2.76 (3)
O(12)	0.1839 (3)	0.0585 (3)	0.1891 (2)	2.84 (7)
O(14)	0.0613 (3)	0.1007 (3)	0.3257 (2)	3.16 (7)
O(22)	0.0725 (3)	0.2109 (3)	0.1807 (2)	3.33 (7)
O(24)	0.2019 (3)	0.3331 (3)	0.3482 (3)	3.75 (8)
C(11)	0.0822 (6)	−0.1330 (6)	0.1173 (5)	5.1 (2)
C(12)	0.0857 (5)	−0.0426 (5)	0.1827 (4)	3.3 (1)
C(13)	−0.0119 (5)	−0.0732 (5)	0.2307 (4)	3.7 (1)
C(14)	−0.0214 (5)	−0.0026 (5)	0.2961 (4)	3.4 (1)
C(15)	−0.1385 (6)	−0.0543 (6)	0.3380 (5)	4.8 (1)
C(21)	−0.0862 (7)	0.2608 (7)	0.1144 (5)	5.7 (2)
C(22)	0.0066 (5)	0.2669 (5)	0.1921 (4)	4.2 (1)
C(23)	0.0171 (6)	0.3318 (6)	0.2668 (5)	4.7 (1)
C(24)	0.1092 (5)	0.3600 (5)	0.3388 (4)	4.0 (1)
C(25)	0.1121 (7)	0.4386 (7)	0.4139 (5)	6.0 (2)
H	0.355 (5)	0.295 (5)	0.312 (4)	1 (1)

[a] Values for atoms refined isotropically. Data for phenyl group atoms are available as supplementary material.

the acac and PPh_3 ligands were calculated by assuming idealized geometry and a C–H distance of 0.95 Å. Also, B(H) was taken as being equal to $1.3[B_{eqv}(C)]$.

Positional parameters and their errors for the non-phenyl group atoms of **1**–**3** are listed in Tables II–IV. Important intramolecular bond distances and angles for **1** are in Table V while those for **2** and **3** are compared in Table VI. Tables giving full details of the crystal data and data collection parameters (Tables S1–S3), the non-hydrogen positional parameters (Tables S4–S6), the positional parameters for the hydrogen atoms (Tables S7–S9), the anisotropic thermal parameters for **1** and **3** (Tables S10 and S11), and complete bond distances (Tables S12–S14) and bond angles (Tables S15–S17) are available as supplementary material, as well as figures (Figures S1–S3) showing the full atomic numbering schemes.

Table IV. Positional Parameters and Equivalent Isotropic Displacement Parameters for Non-Phenyl Atoms of **3** and Their Estimated Standard Deviations

atom	*x*	*y*	*z*	*B*,[a] Å^2
Re	0.06946 (5)	0.23801 (2)	0.06272 (2)	3.350 (9)
P(1)	−0.1061 (3)	0.3030 (1)	0.0954 (2)	3.74 (7)
P(2)	0.0353 (3)	0.1960 (1)	−0.0443 (1)	3.46 (7)
O(32)	0.1470 (8)	0.2653 (4)	0.1480 (4)	4.2 (2)
O(34)	0.1263 (7)	0.3278 (3)	0.0299 (3)	3.6 (2)
O(42)	0.0436 (7)	0.1477 (3)	0.1045 (3)	3.4 (2)
O(44)	0.2543 (7)	0.2063 (4)	0.0506 (4)	4.3 (2)
C(31)	0.303 (2)	0.3033 (9)	0.2221 (8)	7.9 (5)
C(32)	0.238 (1)	0.3065 (7)	0.1579 (6)	4.7 (3)
C(33)	0.272 (1)	0.3564 (6)	0.1144 (7)	5.0 (3)
C(34)	0.214 (1)	0.3659 (6)	0.0560 (6)	4.6 (3)
C(35)	0.244 (2)	0.4269 (7)	0.0165 (7)	6.6 (4)
C(41)	0.077 (2)	0.0526 (6)	0.1696 (7)	6.6 (4)
C(42)	0.129 (1)	0.1100 (6)	0.1316 (6)	5.0 (3)
C(43)	0.255 (1)	0.1162 (6)	0.1254 (6)	5.3 (3)
C(44)	0.310 (1)	0.1600 (7)	0.0839 (7)	5.6 (3)
C(45)	0.450 (2)	0.159 (1)	0.076 (1)	9.9 (6)
P(10)	0.4795 (4)	0.4957 (2)	0.7806 (2)	5.7 (1)
F(1)	0.482 (1)	0.4767 (6)	0.7077 (5)	11.3 (4)
F(2)	0.3324 (9)	0.5024 (6)	0.7723 (6)	10.7 (3)
F(3)	0.466 (1)	0.4197 (4)	0.7960 (6)	10.9 (3)
F(4)	0.478 (1)	0.5141 (8)	0.8496 (5)	14.5 (4)
F(5)	0.491 (1)	0.5712 (5)	0.7626 (7)	13.1 (4)
F(6)	0.623 (1)	0.4884 (7)	0.7870 (7)	12.4 (4)

[a] Values for anisotropically refined atoms are given in the form of the isotropic equivalent thermal parameter defined as $(4/3)[a^2B(1,1) + b^2B(2,2) + c^2B(3,3) + ab(\cos\gamma)B(1,2) + ac(\cos\beta)B(1,3) + bc(\cos\alpha)B(2,3)]$. Data for the phenyl group atoms are available as supplementary material.

Table V. Important Bond Distances (Å) and Bond Angles (deg) for **1**[a]

Bond Distances			
Re–P(1)	2.451 (2)	Re–N(21)	2.131 (7)
Re–P(2)	2.455 (2)	O(171)–C(17)	1.29 (1)
Re–O(171)	2.075 (6)	O(172)–C(17)	1.22 (1)
Re–O(271)	2.066 (6)	O(271)–C(27)	1.30 (1)
Re–N(11)	2.114 (7)	O(272)–C(27)	1.23 (1)
Bond Angles			
P(1)–Re–P(2)	118.20 (8)	O(171)–Re–N(21)	83.3 (3)
P(1)–Re–O(171)	80.4 (2)	O(271)–Re–N(11)	84.0 (3)
P(1)–Re–O(271)	160.4 (2)	O(271)–Re–N(21)	77.6 (3)
P(1)–Re–N(11)	91.0 (2)	N(11)–Re–N(21)	155.4 (3)
P(1)–Re–N(21)	100.9 (2)	O(171)–C(17)–O(172)	125 (1)
P(2)–Re–O(171)	160.7 (2)	O(171)–C(17)–C(12)	115.7 (9)
P(2)–Re–O(271)	81.2 (2)	O(172)–C(17)–C(12)	120 (1)
P(2)–Re–N(11)	96.3 (2)	O(271)–C(27)–O(272)	124 (1)
P(2)–Re–N(21)	96.8 (2)	O(271)–C(27)–C(22)	114.9 (9)
O(171)–Re–O(271)	80.0 (3)	O(272)–C(27)–C(22)	121 (1)
O(171)–Re–N(11)	77.5 (3)		

[a] Numbers in parentheses are estimated standard deviations in the least significant digits.

Physical Measurements. Infrared spectra were recorded as Nujol mulls between KBr plates on a Perkin-Elmer Model 1800 IR Fourier transform (4000–450 cm^{-1}) spectrometer. Electronic absorption spectra were recorded on an IBM Instruments 9420 (900–300 nm) UV–visible spectrophotometer. Electrochemical measurements were carried out by the use of a Bioanalytical Systems Inc. Model CV-1A instrument on dichloromethane or acetonitrile solutions that contained 0.1 M tetra-*n*-butylammonium hexafluorophosphate (TBAH) as the supporting electrolyte. $E_{1/2}$ values, determined as $(E_{p,a} + E_{p,c})/2$, were referenced to the silver/silver chloride (Ag/AgCl) electrode at room temperature and are uncorrected for junction potentials. Under our experimental conditions, the ferrocenium/ferrocene couple is at $E_{1/2} = +0.47$ V vs Ag/AgCl. ^{1}H NMR spectra were recorded on a Varian XL-200 spectrometer. Resonances were referenced internally to the residual protons in the incompletely deuteriated solvent. ^{31}P{^{1}H} NMR were obtained on a Varian XL-200 spectrometer. An internal deuterium lock and an external reference, 85% H_3PO_4, were used. Conductivity measurements were performed on acetone or acetonitrile solutions of the samples at a concentration of ca. 1.0×10^{-3} M. Measurements were made with the

Table VI. Comparison of Important Bond Distances (Å) and Bond Angles (deg) for **2** and **3**[a]

2		3	
	Bond Distances		
Re-P(1)	2.334 (1)	Re-P(1)	2.396 (3)
Re-P(2)	2.342 (1)	Re-P(2)	2.439 (3)
Re-O(12)	2.079 (3)	Re-O(34)	2.013 (6)
Re-O(14)	2.103 (3)	Re-O(32)	2.036 (7)
Re-O(22)	2.116 (3)	Re-O(44)	2.092 (7)
Re-O(24)	2.092 (3)	Re-O(42)	2.022 (6)
Re-H	1.54 (5)		
	Bond Angles		
P(1)-Re-P(2)	110.35 (4)	P(1)-Re-P(2)	111.6 (1)
P(1)-Re-O(12)	83.53 (9)	P(1)-Re-O(34)	82.9 (2)
P(1)-Re-O(14)	87.39 (9)	P(1)-Re-O(32)	83.7 (2)
P(1)-Re-O(22)	159.2 (1)	P(1)-Re-O(44)	161.1 (2)
P(1)-Re-O(24)	104.6 (1)	P(1)-Re-O(42)	103.0 (2)
P(1)-Re-H	64 (2)		
P(2)-Re-O(12)	87.68 (9)	P(2)-Re-O(34)	90.7 (2)
P(2)-Re-O(14)	161.32 (9)	P(2)-Re-O(32)	164.3 (2)
P(2)-Re-O(22)	83.26 (9)	P(2)-Re-O(44)	83.4 (2)
P(2)-Re-O(24)	102.4 (1)	P(2)-Re-O(42)	95.3 (2)
P(2)-Re-H	65 (2)		
O(12)-Re-O(14)	88.6 (1)	O(32)-Re-O(34)	87.6 (3)
O(12)-Re-O(22)	81.4 (1)	O(34)-Re-O(44)	85.6 (3)
O(12)-Re-O(24)	163.6 (1)	O(34)-Re-O(42)	169.3 (3)
O(12)-Re-H	123 (2)		
O(14)-Re-O(22)	78.1 (1)	O(32)-Re-O(44)	80.9 (3)
O(14)-Re-O(24)	77.7 (1)	O(32)-Re-O(42)	84.2 (3)
O(14)-Re-H	131 (2)		
O(22)-Re-O(24)	86.9 (1)	O(42)-Re-O(44)	86.3 (3)
O(22)-Re-H	137 (2)		
O(24)-Re-H	73 (2)		

[a] Data have been arranged so as to compare related distances and angles between the two structures. Numbers in parentheses are estimated standard deviations in the least significant digits.

use of an Industrial Instruments Inc. Model RC-16B2 conductivity bridge. EPR spectra of CH_2Cl_2 or acetone/toluene glasses were recorded at ca. −160 °C with a Varian E-109 spectrometer.

Analytical Procedures. Elemental microanalyses were performed by Dr. H. D. Lee of the Purdue University Microanalytical Laboratory.

Results and Discussion

The heptahydride complex $ReH_7(PPh_3)_2$ reacts with the ligands pyridine-2-carboxylic acid (picolinic acid, picH), 1-isoquinolinecarboxylic acid (isoquinH), pyridine-2,3-dicarboxylic acid (quinH), and acetylacetone (acacH) in ethanol, and with 2-hydroxypyridine (Hhp) and 2-hydroxy-6-methylpyridine (Hmhp) in acetone, to afford the monohydridorhenium(III) complexes $ReH(A)_2(PPh_3)_2$, where A represents the chelating monoanionic ligand derived from the aforementioned organic acids. The product yields were at least 70%. In contrast, the much more kinetically inert pentahydrides $ReH_5(PPh_3)_3$ and $ReH_5(PPh_3)_2(py)$ failed to react with picolinic acid in refluxing ethanol, THF, or 1,2-dichloroethane. Further reactions with these pentahydrides were not examined.

(a) Properties of the Heterocyclic Carboxylate Complexes. These intensely colored (red-purple) complexes[8] dissolved in acetonitrile to give solutions (ca. 1×10^{-3} M) that were essentially nonconducting, with Λ_m values in the range 2–10 Ω^{-1} cm^2 mol^{-1}. The IR spectra of Nujol mulls showed a weak ν(Re–H) mode only in the case of $ReH(pic)_2(PPh_3)_2$ (2117 cm^{-1}) and $ReH(isoquin)_2(PPh_3)_2$ (2078 cm^{-1}). In all cases, IR spectroscopy also supported the formulation of these complexes as containing water of crystallization. Otherwise, the IR spectra were not especially helpful in establishing the identity and purity of these products, other than in revealing the presence of strong bands associated with the ν(COO) modes in the region from 1710 to 1600 cm^{-1}. In the case of $ReH(quin)_2(PPh_3)_2$, there is also a very strong, broad band centered at 1520 cm^{-1} that probably arises from the uncomplexed carboxylic acid group.

The ^{1}H NMR spectrum of each complex (measured in CD_2Cl_2) consists of a fairly complex set of phenyl proton resonances around δ +7.2, and a triplet at ca. δ −3 that is assignable to the Re–*H* resonance that exhibits coupling to the phosphorus atoms of the two PPh_3 ligands. The chemical shift values for Re–*H* and the P–H coupling constants of ca. 70 Hz (Table VII) are characteristic of seven-coordinate monohydridorhenium(III) complexes.[1] In the case of $ReH(quin)_2(PPh_3)_2$, the pyridyl group proton resonances are easily distinguishable from those of the phenyl rings. A doublet of doublets at δ +6.58 is associated with the 5-proton on the pyridyl group. There are also two doublets centered at δ +8.42 (J = 8.1 Hz) and δ +8.30 (J = 5.8 Hz); these are due to the inequivalent 4,6-protons on the pyridyl ring that are split by coupling to the 5-proton. Each of these doublets shows further splitting that arises through coupling between the 4- and 6-protons themselves ($J \simeq$ +1.3 Hz). A singlet at δ +17.5 is assigned to the proton on the free carboxylic acid group at the 3-position. Integration is in accord with the proposed stoichiometry of this complex. All three complexes show a singlet in their $^{31}P\{^1H\}$ NMR spectra (Table VII). In the case of $ReH(pic)_2(PPh_3)_2$, the ^{31}P NMR spectrum is a doublet (J_{P-H} = 67 Hz), thereby confirming the presence of a single hydride ligand.

The electrochemical properties of these complexes are similar. Cyclic voltammetric (CV) measurements on solutions of $ReH(pic)_2(PPh_3)_2$ in 0.1 M TBAH/CH_2Cl_2 show a reversible couple at $E_{1/2}$ = +0.26 V vs Ag/AgCl that corresponds to a one-electron oxidation of the complex and an irreversible oxidation at $E_{p,a}$ = +1.44 V. CV measurements on solutions of $ReH(isoquin)_2(PPh_3)_2$ and $ReH(quin)_2(PPh_3)_2$ show analogous processes to those mentioned above (see Table VII), as well as a reversible reduction below −1.3 V. The complex $ReH(pic)_2(PPh_3)_2$ has been electrochemically oxidized (at +0.40 V) to generate solutions containing the orange monocation; this species can be electrochemically reduced back to the starting complex upon bulk electrolysis at ca. +0.05 V. For the pyridinecarboxylate complexes $ReH(pic)_2(PPh_3)_2$ and $ReH(isoquin)_2(PPh_3)_2$, this oxidation can be accessed with the use of the one-electron oxidant $[(\eta^5\text{-}C_5H_5)_2Fe]PF_6$ in acetone. The resulting complexes, $[ReH(pic)_2(PPh_3)_2]PF_6$ (orange) and $[ReH(isoquin)_2(PPh_3)_2]PF_6$ (dark blue), can be reduced back to their neutral precursors by the use of solutions of cobaltocene in acetone. The oxidized derivatives have very similar electrochemical properties to the neutral precursors, except that the process at $E_{1/2}$ ca. +0.2 V is now a reduction. This suggests that little structural rearrangement has occurred as a result of the electron transfer. In the case of the picolinate derivative, its IR spectrum shows a sharp ν(Re–H) mode at 2085 (w) cm^{-1}; the spectra of both complexes show an intense band at ca. 840 cm^{-1} due to ν(P–F) of PF_6^-.

Toluene/acetone solutions (1:1) of $[ReH(pic)_2(PPh_3)_2]PF_6$ are ESR-active at low temperatures (−160 °C). The X-band spectrum shows a broad signal spanning the range 1.6–3.3 kG and centered at g = 2.58. The paramagnetism of this complex and its isoquin analogue was confirmed by magnetic moment determinations on dichloromethane solutions using the Evans method:[9] μ_{eff} = 1.7 (±0.1) μ_B for $[ReH(pic)_2(PPh_3)_2]PF_6$ and μ_{eff} = 1.5 (±0.1) μ_B for $[ReH(isoquin)_2(PPh_3)_2]PF_6$.

The first oxidation of $ReH(quin)_2(PPh_3)_2$ is at a potential ($E_{1/2}$ = +0.54 V) more positive than that of the $[(\eta^5\text{-}C_5H_5)_2Fe]^+/(\eta^5\text{-}C_5H_5)_2Fe$ couple ($E_{1/2}$ = +0.47 vs Ag/AgCl). The use of $NOPF_6$ as an alternative oxidant (in acetone) gave an orange product that did not contain $[ReH(quin)_2(PPh_3)_2]^+$ as evidenced by cyclic voltammetry on solutions in 0.1 M TBAH/CH_3CN ($E_{1/2}$ = +1.27 V vs Ag/AgCl). While the identity of this product has not been established, it does not appear to be a hydride complex since no Re–*H* resonance was seen in its ^{1}H NMR spectrum

(8) The electronic absorption spectral data for these complexes (recorded in CH_2Cl_2) are as follows (λ_{max} values are quoted and molar extinction coefficients are given in parentheses): $ReH(pic)_2(PPh_3)_2$, 507 (8900), 420 sh, 357 (6200); $ReH(isoquin)_2(PPh_3)_2$, 598 (13 800), 510 sh, 330 (14 800); $ReH(quin)_2(PPh_3)_2$, 533 (8100), 484 (8200), 310 (5600). Futher information concerning these spectra and the electronic absorption spectra of the other complexes described in this report can be obtained from R.A.W.

(9) Evans, D. F. *J. Chem. Soc.* **1959**, 2003.

Table VII. NMR Spectra and Electrochemical Properties of $ReH(A)_2(PPh_3)_2$

complex	^1H NMR,[a] δ Re-*H*[b]	$^{31}P\{^1H\}$NMR,[a] δ	CV half-wave potential,[c] V $E_{p,a}$	$E_{1/2}$(ox)	$E_{1/2}$(red)
$ReH(pic)_2(PPh_3)_2 \cdot H_2O$	−3.06 (69)	+25.2[e]	+1.44	+0.26 (100)	
$ReH(isoquin)_2(PPh_3)_2 \cdot H_2O$	−2.90 (70)	+24.4	+1.33	+0.21 (100)	−1.64 (120)
$ReH(quin)_2(PPh_3)_2 \cdot H_2O$	−2.65 (67)	+24.0	+1.62	+0.54 (100)	−1.36 (100)
$ReH(hp)_2(PPh_3)_2 \cdot 2H_2O$	−3.63 (61)	+32.1[e]	+1.10	+0.02 (110)	
$ReH(mhp)_2(PPh_3)_2 \cdot H_2O$	−3.33 (64)	+28.5[e]	+1.30	−0.09 (110)	
$ReH(acac)_2(PPh_3)_2$	+4.99 (72)[d]	+34.0[d,e]	+0.85 (120)[f]	−0.44 (110)	

[a] Recorded in CD_2Cl_2 unless otherwise stated. [b] Binomial triplet; J_{P-H} in Hz given in parentheses. [c] Measured on 0.1 M TBAH/CH_2Cl_2 solutions and referenced to the Ag/AgCl electrode, with scan rate (v) of 200 mV s^{-1} at a Pt-bead electrode. Numbers in parentheses are the $E_{p,a} - E_{p,c}$ values in mV. [d] Recorded in C_6D_6. [e] The corresponding ^{31}P NMR spectrum shows that this resonance is split into a doublet; J_{P-H} is in the range 62–71 Hz. [f] This process (corresponding to an oxidation) is reversible; the $E_{1/2}$ value is given.

(recorded in CD_3CN) between δ 0 and −10. Electrochemical oxidation of purple $ReH(quin)_2(PPh_3)_2$ to orange $[ReH(quin)_2(PPh_3)_2]^+$ in 0.2 M TBAH/CH_2Cl_2 can be accomplished at +0.75 V vs Ag/AgCl.

(b) Properties of the Hydroxypyridine Derivatives. The reactions of $ReH_7(PPh_3)_2$ with Hhp and Hmhp in acetone give orange products, $ReH(hp)_2(PPh_3)_2$ and $ReH(mhp)_2(PPh_3)_2$, whose NMR spectra and electrochemical properties (Table VII) resemble closely those of their pic, isoquin, and quin analogues and need not be discussed further. The only exception is the ^1H NMR spectrum of $ReH(mhp)_2(PPh_3)_2$, which, in addition to the phenyl, pyridyl, and Re–*H* resonances, shows a singlet at δ +1.18 due to the methyl group on the pyridyl ring.

Both complexes form solutions in acetone that are essentially nonconducting with $\Lambda_m \simeq 5\ \Omega^{-1}\ cm^2\ mol^{-1}$ for $c_m = 1 \times 10^{-3}$ M. Their IR spectra (Nujol mulls) show weak ν(Re–H) bands at 2054 and 2124 cm^{-1} for the hp and mhp complexes, respectively, and broad ν(O–H) bands due to lattice water.

The complex $ReH(mhp)_2(PPh_3)_2$ has been chemically oxidized to the purple monocation $[ReH(mhp)_2(PPh_3)_2]PF_6$ with the use of $[(\eta^5\text{-}C_5H_5)_2Fe]PF_6$ as the oxidant. The electrochemical properties of this complex are very similar to that of the neutral precursor, except that the process at $E_{1/2} = -0.09$ V is now a reduction. Once again, this suggests that little structural change has occurred as a result of the oxidation. The monocation can in turn be reduced back to the neutral species with the use of the one-electron reductant $(\eta^5\text{-}C_5H_5)_2Co$. Its IR spectrum (Nujol mull) exhibits a ν(Re–H) mode at 2074 (w) cm^{-1} and ν(P–F) of the PF_6^- anion at 840 (s) cm^{-1}. Conductivity measurements on solutions of $[ReH(mhp)_2(PPh_3)_2]PF_6$ in acetone ($c_m = 1 \times 10^{-3}$ M) confirm it to be a 1:1 electrolyte ($\Lambda_m \simeq 110\ \Omega^{-1}\ cm^2\ mol^{-1}$). Additional characterization of this complex have been complicated by its rapid decomposition in solution; this behavior is being investigated further, and the results will be reported in due course. All attempts to isolate a pure sample of the oxidized hp complex $[ReH(hp)_2(PPh_3)_2]PF_6$ have been unsuccessful. Apparently, it is even more unstable than its mhp analogue.

(c) Properties of the Acetylacetonate Derivatives. The complex $ReH(acac)_2(PPh_3)_2 \cdot H_2O$ is a red-brown solid that is soluble in acetone, THF, and dichloromethane and slightly soluble in diethyl ether. The IR spectrum (Nujol mull) of this complex shows characteristic ν(C–O) and ν(C–C) bands of chelating acetylacetonate ligands at 1556 (s) and 1514 (vs) cm^{-1} and a sharp ν(Re–H) band at 2044 (w) cm^{-1}.

The ^1H NMR spectrum of the complex (recorded in C_6D_6) shows phenyl resonances centered at δ +7.5, a singlet at δ +5.04 that is due to the unique C–H proton of each acac ligand, and two singlets of equal intensity at δ +1.98 and δ +1.83, which are attributable to the protons of inequivalent methyl groups; this is consistent with the results of the X-ray crystallographic structure determination of the complex (vide infra). The most surprising feature in the ^1H NMR spectrum is the chemical shift of the Re–*H* resonance (δ +4.99). It is way downfield of the corresponding resonances in the spectra of the other monohydrido complexes (Table VII); this may signal a greater acidic character of this hydrogen in the acac derivative. The $^{31}P\{^1H\}$ and ^{31}P NMR spectra of this complex are similar to those exhibited by the other monohydride complexes listed in Table VII.

The electrochemical behavior of this complex differs somewhat from that exhibited by the other rhenium complexes of similar stoichiometry (Table VII). CV measurements on 0.1 M TBAH/CH_2Cl_2 solutions of $ReH(acac)_2(PPh_3)_2$ show two reversible oxidations, at $E_{1/2} = +0.85$ V and $E_{1/2} = -0.44$ V vs Ag/AgCl. The most accessible of these oxidations (that at $E_{1/2} = -0.44$ V) shows that this complex is much more readily oxidized than the other monohydrido derivatives (Table VII), in accord with the metal center in this complex being more electron rich. This is, in turn, consistent with the downfield shift of the Re–*H* resonance (vide supra).

The neutral acetylacetonate complex can be oxidized electrochemically (at ca. 0 V) to the red monocation. This monocation has electrochemistry similar to that of the neutral precursor, except that the couple at $E_{1/2} = -0.44$ V is now a reduction. Again, the similarities in the electrochemical properties suggest that the neutral and the monocationic species have very similar structures. The subsequent rereduction of the monocation is easily accomplished at a potential of ca. −0.7 V. This oxidation and reduction can be accomplished chemically with the use of the one-electron oxidant $[(\eta^5\text{-}C_5H_5)_2Fe]PF_6$ and reductant $(\eta^5\text{-}C_5H_5)_2Co$, respectively.

The one-electron-oxidized complex $[ReH(acac)_2(PPh_3)_2]PF_6$ is expected to be paramagnetic, and in accord with this, we find $\mu_{eff} = 1.7\ (\pm 0.1)\ \mu_B$ for a dichloromethane solution of this complex (as determined by the Evans method).[9] Dichloromethane solutions of $[ReH(acac)_2(PPh_3)_2]PF_6$ and of the electrochemically oxidized monocation display the same X-band ESR spectrum at low temperature (−160 °C). The spectrum spans the range 2.0–5.3 kG; the most intense component of the complex pattern is centered at $g \simeq 2.7$. Conductivity measurements on an acetone solution of this complex ($c_m = 1 \times 10^{-3}$ M) confirmed it to be a 1:1 electrolyte ($\Lambda_m = 125\ \Omega^{-1}\ cm^2\ mol^{-1}$). Its IR spectrum (Nujol mull) is similar to that of the neutral derivative, with the exception of a ν(P–F) mode at 842 (s) cm^{-1} and a shift in ν(Re–H) to 1970 (w) cm^{-1}.

(d) X-ray Crystal Structure Determinations of $[ReH(pic)_2(PPh_3)_2]PF_6$ (1), $ReH(acac)_2(PPh_3)_2$ (2), and $[ReH(acac)_2(PPh_3)_2]PF_6$ (3). The ORTEP representations of the structures of the seven-coordinate cations of **1** and **3** and the neutral complex **2** are shown in Figures 1–3. The important intramolecular bond distances and bond angles are given in Tables V and VI. A simple comparison between the structures is shown in Figure 4. In each case, the structures are represented (for convenience) schematically in terms of a distorted pentagonal-bipyramidal geometry, with the two phosphorus atoms and two of the oxygen atoms constituting four of the five ligand atoms of the "pentagonal plane".[10] The two axial ligand atoms are the nitrogen atoms of the picolinate ligands in the case of **1** and oxygen atoms of the acac ligands for **2** and **3**. Relatively small differences between these structures can be seen in a comparison of the bond angles. For example,

(10) This description is of course an approximation since, with such disparate sets of ligands, significant deviations from an ideal geometry are to be expected. Least-squares planes calculations for the "pentagonal planes" in **1**–**3** (excluding the hydrido ligands) show that the largest displacements of any of the four ligand atoms that form the planes are as follows: 0.034 (6) Å for O(171) of **1**; 0.132 (4) Å for O(22) of **2**; 0.102 (7) Å for O(32) of **3**.

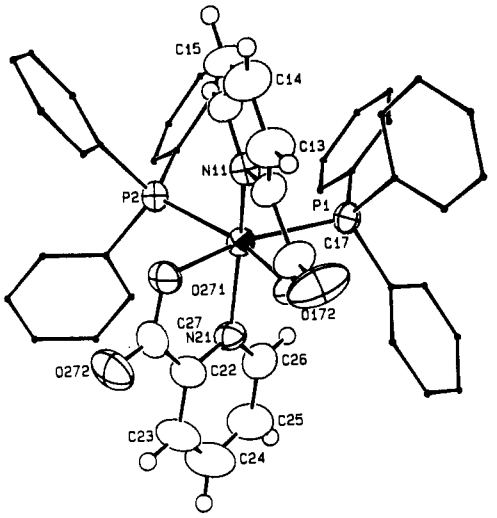

Figure 1. ORTEP representation of the rhenium-containing cation of **1** showing the atomic numbering scheme for the non-phenyl atoms. The thermal ellipsoids are drawn at the 50% probability level. The Re–H bond is probably located in the void defined by the ligand set P(2), P(1), and N(21).

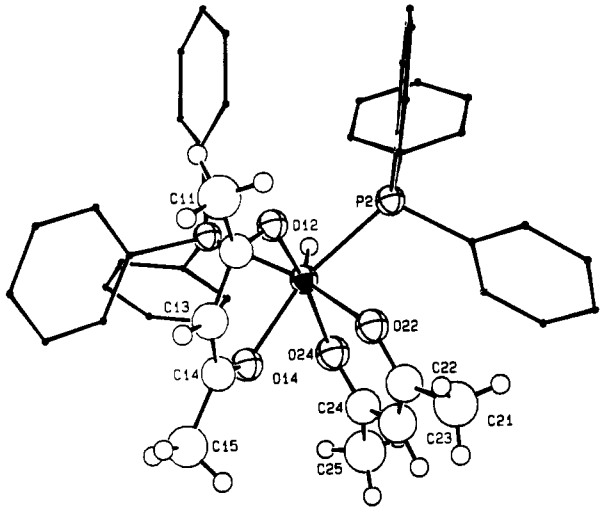

Figure 2. ORTEP representation of **2** showing the atomic numbering scheme for the non-phenyl atoms. The thermal ellipsoids are drawn at the 50% probability level.

within the "pentagonal plane", the P(1)–Re–P(2) angle varies from 118.20 (8)° (for **1**), to 110.35 (4)° (for **2**), to 111.6 (1)° (for **3**), whereas for the corresponding O–Re–O angles the change is much smaller, viz., 80.0 (3)° [O(171)–Re–O(271) for **1**], 78.1 (1)° [O(14)–Re–O(22) for **2**], and 80.9 (3)° [O(32)–Re–O(44) for **3**]. The angles involving the trans axial Re–ligand bonds are as follows: **1**, N(11)–Re–N(21) = 155.4 (3)°; **2**, O(12)–Re–O(24) = 163.6 (1)°; **3**, O(34)–Re–O(42) = 169.3 (3)°. The much smaller angle for the picolinate complex **1** is presumably a consequence of constraints imposed by the rather rigid picolinate ligand in forming the five-membered chelate rings; this can be contrasted with the corresponding six-membered rings formed in the case of **2** and **3**.

The hydride ligand was located only in the case of the neutral acetylacetone complex **2**, but a similar disposition of the hydride ligand is likely in the case of **1** and **3** because of the close similarities in the ligand orientations in these three structures. The hydride ligands are therefore located where the angular distortions associated with the other six ligand atoms generate the largest void in the metal coordination sphere. The hydride ligand in **2** is located below the "pentagonal plane" as defined in Figure 4. This is reflected by the disparity in the appropriate H–Re–O angles, which are 123 (2)° [H–Re–O(12)] and 73 (2)° [H–Re–O(24)]. Accordingly, the description of these structures in terms

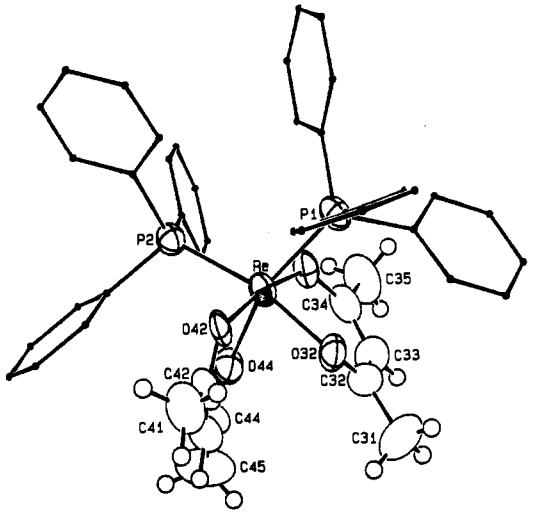

Figure 3. ORTEP representation of the rhenium-containing cation of **3** showing the atomic numbering scheme for the non-phenyl atoms. The thermal ellipsoids are drawn at the 50% probability level. This orientation shows clearly the most likely location of the hydride ligand, namely, in the face defined by the ligand set P(2), P(1), and O(34).

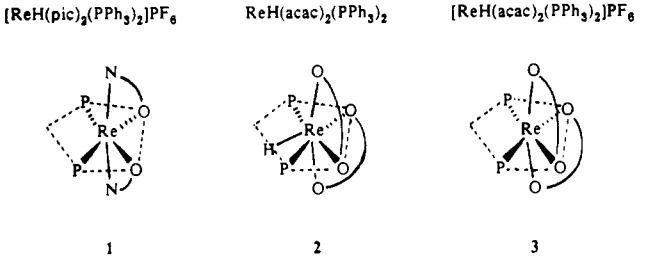

Figure 4. Comparison of the structures of **1**–**3** in terms of distorted-pentagonal-bipyramidal geometries. An alternative description in terms of face-capped octahedra is also possible (see text).

of face-capped octahedra may be preferable to that of distorted pentagonal bipyramids.

The structures of **2** and **3** are very similar as seen from a comparison in the bond distances and angles given in Table VI. This result is in accord with the electrochemical properties of the complexes which demonstrate the reversibility of the +/0 couple; this implies that only minor structural changes will accompany the electron transfer, and this is seen to be the case. The Re–P bond distances of **2** (2.334 (1) and 2.342 (1) Å) are shorter than those of **3** (2.396 (3) and 2.439 (3) Å), a difference that may reflect a greater Re → P π-back-bonding contribution in the lower valent complex **2**. The difference in Re–O bond lengths is in the opposite order and accords with the Re–O bonds being more influenced by electrostatic factors; the shorter bonds are associated with the more highly charged (higher oxidation state) metal center in **3**. The angular distortions are rather small, the largest difference being ca. 7° between O(14)–Re–O(24) of 77.7 (1)° and O(32)–Re–O(42) of 84.2 (3)°.

(e) Concluding Remarks. The present study shows not only that various organic acids react very readily with $ReH_7(PPh_3)_2$ to afford diamagnetic, seven-coordinate monohydridorhenium(III) complexes but that the latter species are easily oxidized to their stable, paramagnetic, rhenium(IV) congeners. NMR spectroscopy, cyclic voltammetry, and X-ray crystallography have been used to establish the structural identity of these complexes. This work establishes that the previous rarity of mononuclear rhenium(IV) hydride complexes[2] cannot be attributed to their inherent instability. The only previous report of mononuclear rhenium hydride complexes that contain phosphine and acetylacetonate ligands is one by Freni et al.;[11] this describes the isolation of $ReH_2(acac)(PPh_3)_3$, $ReHX(acac)(PPh_3)_3$, and $ReHX_2(acac)(PPh_3)_2$

(11) Freni, M.; Romiti, P.; Guisto, D. *J. Inorg. Nucl. Chem.* **1970**, *32*, 145.

(X = Cl, Br, I). Our isolation and characterization of the redox pair $ReH(acac)_2(PPh_3)_2$ and $[ReH(acac)_2(PPh_3)_2]PF_6$ provides further important examples and the first complete structural characterization of such derivatives.

Acknowledgment. Support from the National Science Foundation, through Grant No. CHE88-07444 to R.A.W. and Grant No. CHE86-15556 for the purchase of the MicroVAX II computer and diffractometer, is gratefully acknowledged. We also acknowledge the National Institutes of Health (Grant No. RR-01077) and the National Science Foundation (Grant No. 87-14258) for funds for the purchase of the NMR spectrometers.

Supplementary Material Available: Tables giving full details of the crystal data and data collection parameters for **1-3** (Table S1-S3), non-hydrogen positional parameters for **1-3** (Tables S4-S6), positional parameters for the hydrogen atoms of **1-3** (Tables S7-S9), anisotropic thermal parameters for **1** and **3** (Tables S10 and S11), and complete bond distances (Tables S12-S14) and bond angles (Tables S15-S17) for **1-3** and figures (Figures S1-S3) showing the full atomic numbering schemes for **1-3** (46 pages); tables of observed and calculated structure factors (91 pages). Ordering information is given on any current masthead page.

Contribution from the Sterling Chemistry Laboratory,
Yale University, New Haven, Connecticut 06511-8118

Planar Tricoordinate Oxygens in a Mixed Aqua(tetrahydrofuran)iridium Complex: X-ray Crystal and Molecular Structure of $[IrH_2(THF)(H_2O)(PPh_3)_2]SbF_6 \cdot THF$

Xiao-Liang Luo, Gayle K. Schulte, and Robert H. Crabtree*

Received June 7, 1989

The hydrogenation of $[(cod)Ir(PPh_3)_2]SbF_6$ in tetrahydrofuran (THF) gives $[IrH_2(THF)_2(PPh_3)_2]SbF_6$ (**1**). $[IrH_2(THF)(H_2O)(PPh_3)_2]SbF_6$ (**2**) is formed on recrystallization of **1** from moist THF/hexane. The crystal structure of **2**·THF has been determined by a single-crystal X-ray diffraction study. This is one of the rare crystallographically characterized examples of THF and of water binding to a late d-block transition metal. **2**·THF crystallizes in the space group $P2_1/n$ with a = 10.745 (4) Å, b = 18.793 (8) Å, c = 22.425 (8) Å, β = 96.42 (3)°, V = 4500 (6) Å^3, Z = 4, and ρ_{calcd} = 1.64 g/cm^3. The structure was refined by full-matrix least-squares techniques to a final R factor of 0.039 for 3666 reflections. One THF and one H_2O molecule occupy two cis sites of the octahedron around the iridium(III) center. The phosphines are trans with Ir-P(av) of 2.298 (3) Å. The Ir-O bond distances are 2.305 (9) and 2.258 (9) Å, significantly longer than are expected in the absence of the trans influence of the hydride ligands. The coordinated THF ligand is reasonably well-defined and adopts an envelope conformation with C(3) on the flap atom; the tricoordinate oxygen atom is in a planar configuration, in contrast to the commonly observed pyramidal configuration. The aqua ligand is hydrogen-bonded to an F atom of the SbF_6 counterion and to the oxygen of the lattice THF. The approximate positions of the H atoms constituting the H-bonds were deduced from the heavy-atom positions by using the Ferraris-Franchini-Angela correlations. These are consistent with the H_2O ligand also having a planar rather than a pyramidal oxygen. Arguments about π-bonding and 2-e vs 4-e donor character for ligands of the R_2O type should therefore not be simply based on the distinction between planar and pyramidal geometries.

Introduction

Transition-metal solvento complexes, which contain weakly coordinated solvent molecules as ligands, are of great importance.[1] They have been proposed to be the intermediates in many homogeneous catalytic processes.[2] The facile dissociation of the labile solvent molecules can create vacant coordination sites required for substrate binding and activation. Indeed, many isolable solvento complexes have shown catalytic activity in a variety of reactions[3-8] including C-H activation.

In spite of its importance as a ligand, the structural chemistry of coordinated H_2O has received relatively little attention in organometallic, as opposed to coordination, compounds. These two classes of aqua complex may prove to have similar structural chemistries, but evidence has been lacking up to now. In coordination compounds, neutron diffraction has usually been necessary to allow secure conclusions to be drawn. It has been found[9] that coordinated H_2O retains the H-O-H angle of 107°, characteristic of the free molecule, showing that the sp^3 hybridization is retained on binding. Both protons on the H_2O often form H-bonds in the crystal. Surprisingly, metal ions coordinate apparently indiscriminantly in the plane of the lone pairs, so that both planar and pyramidal configurations are found for the three-coordinate oxygen of bound H_2O, as well as intermediate forms. In the planar form, neither of the lone pairs on oxygen is pointing directly at the metal, and the structure disobeys the Nyholm-Gillespie rules. A possible explanation for the common occurrence of the planar form is that the bonding in the structures which have been studied (e.g., $MnCl_2(H_2O)_4$, $Cu(H_2O)_5(SO_4)$) is predominantly ionic. The first question, therefore, is whether the tendency for oxygen to be planar is also manifested in 18-e organometallic species, where we expect more covalent character in the bond.

(1) (a) Davies, J. A.; Hartley, F. R. *Chem. Rev.* **1981**, *81*, 79. (b) Crabtree, R. H.; Demou, P. C.; Eden, D.; Mihelcic, J. M.; Parnell, C. A.; Quirk, J. M.; Morris, G. E. *J. Am. Chem. Soc.* **1982**, *104*, 6994. (c) Crabtree, R. H.; Davis, M. W.; Mellea, M. F.; Mihelcic, J. M. *Inorg. Chim. Acta* **1983**, *72*, 223. (d) Crabtree, R. H.; Hlatky, G. G.; Parnell, B. E.; Segmuller, B. E.; Uriarte, R. J. *Inorg. Chem.* **1984**, *23*, 354. (e) Rhodes, L. F.; Zubkowski, J. D.; Folting, K.; Huffman, J. C.; Caulton, K. G. *Inorg. Chem.* **1982**, *21*, 4185. (f) Bruno, J. W.; Huffman, J. C.; Caulton, K. G. *J. Am. Chem. Soc.* **1984**, *106*, 1663. (g) Allison, J. D.; Moehring, G. A.; Walton, R. A. *J. Chem. Soc., Dalton Trans.* **1986**, 67. (h) Moehring, G. A.; Walton, R. A. *J. Chem. Soc., Dalton Trans.* **1987**, 715.

(2) (a) James, B. R. *Adv. Organomet. Chem.* **1979**, *17*, 319. (b) Halpern, J. *Inorg. Chim. Acta* **1981**, *50*, 11. (c) Backvall, J. E.; Akermark, B.; Ljunggren, S. O. *J. Am. Chem. Soc.* **1979**, *101*, 2411. (d) Stille, J. K.; Divakaruni, R. *J. Organomet. Chem.* **1979**, *169*, 239.

(3) (a) Shapley, J. R.; Schrock, R. R.; Osborn, J. A. *J. Chem. Soc. Soc.* **1969**, *91*, 2816. (b) Schrock, R. R.; Osborn, J. A. *J. Am. Chem. Soc.* **1976**, *98*, 2134. (c) Schrock, R. R.; Osborn, J. A. *J. Am. Chem. Soc.* **1976**, *98*, 2143. (d) Schrock, R. R.; Osborn, J. A. *J. Am. Chem. Soc.* **1976**, *98*, 4450.

(4) (a) Crabtree, R. H.; Mellea, M. F.; Mihelcic, J. M.; Quirk, J. M. *J. Am. Chem. Soc.* **1982**, *104*, 107. (b) Crabtree, R. H.; Parnell, C. P. *Organometallics* **1984**, *3*, 1727. (c) Burk, M. J.; Crabtree, R. H.; Parnell, C. P.; Uriarte, R. J. *Organometallics* **1984**, *3*, 816. (d) Crabtree, R. H.; Parnell, C. P.; Uriarte, R. J. *Organometallics* **1987**, *6*, 696. (e) Luo, X.-L.; Crabtree, R. H. *J. Am. Chem. Soc.* **1989**, *111*, 2527.

(5) (a) Davies, J. A.; Hartley, F. R.; Murray, S. G. *Inorg. Chem.* **1980**, *19*, 2299. (b) Davies, J. A.; Hartley, F. R.; Murray, S. G. *J. Chem. Soc., Dalton Trans.* **1980**, 2246. (c) Davies, J. A.; Hartley, F. R.; Murray, S. G. *J. Mol. Catal.* **1981**, *10*, 171.

(6) Roper, M.; He, R.; Schieren, M. *J. Mol. Catal.* **1985**, *31*, 335.

(7) (a) Sen, A.; Lai, T.-W. *J. Am. Chem. Soc.* **1981**, *103*, 4627. (b) Sen, A.; Lai, T.-W. *Organometallics* **1982**, *1*, 415. (c) Sen, A.; Thomas, R. R. *Organometallics* **1982**, 1251.

(8) Conelly, N. G.; Draggett, P. T.; Green, M. *J. Organomet. Chem.* **1977**, *140*, C10. Thomas, B. J.; Theopold, K. H. *J. Am. Chem. Soc.* **1988**, *110*, 5902.

(9) Ferraris, G.; Franchini-Angela, M. *Acta Crystallgr.* **1972**, *B28*, 3572.

0020-1669/90/1329-0682$02.50/0